Causal relationship between the right auditory cortex and speech-evoked frequency-following response: Evidence from combined tDCS and EEG

Guangting Mai[1,*], Peter Howell[1,*]

[1]Department of Experimental Psychology, University College London, London, UK, WC1H 0AP

***Correspondence:** guangting.mai.15@ucl.ac.uk (G.M.); p.howell@ucl.ac.uk (P.H.)

Abbreviated title: Causal relation between auditory cortex and FFR

Conflict of interest: The authors declare no competing financial interests

Author contributions: G.M. designed research, performed research, and analysed the data; P.H. provided laboratory resources and supervised the study; G.M. drafted the manuscript; both authors contributed to writing, editing and approving the paper.

Acknowledgments: We thank Dr Naheem Bashir for instructions on tDCS experiment setups and Mr Andrew Clark for technical support for EEG experiments. We also thank the Dominic Barker Trust who paid for the tDCS equipment. G.M. was supported by a UCL Graduate Research Scholarship for Cross-disciplinary Training.

Abstract

Speech-evoked frequency-following response (FFR) reflects the neural encoding of speech periodic information in the human auditory systems. FFR is of fundamental importance for pitch and speech perception and serves as clinical biomarkers for various auditory and language disorders. While it is suggested that the main neural source of FFR is in the auditory brainstem, recent studies have shown a cortical contribution to FFR predominantly in the right hemisphere. However, it is still unclear whether auditory cortex and FFR are causally related. The aim of this study was to establish this causal relationship using a combination of transcranial direct current stimulation (tDCS) and scalp-recorded electroencephalography (EEG). We applied tDCS over the left and right auditory cortices in right-handed normal-hearing participants and examined the after-effects of tDCS on FFR using EEG during monaural listening to a repeatedly-presented speech syllable. Our results showed that: (1) before tDCS was applied, participants had greater FFR magnitude when they listened to speech from the left than the right ear, illustrating right-lateralized hemispheric asymmetry for FFR; (2) anodal and cathodal tDCS applied over the right, but not left, auditory cortex significantly changed FFR magnitudes compared to the sham stimulation; specifically, such after-effects occurred only when participants listened to speech from the left ear, emphasizing the right auditory cortical contributions along the contralateral pathway. The current finding thus provides the first causal evidence that validates the relationship between the right auditory cortex and speech-evoked FFR and should significantly extend our understanding of speech encoding in the brain.

Significance Statement

Speech-evoked frequency-following response (FFR) is a neural activity that reflects the brain's encoding of speech periodic features. The FFR has great fundamental and clinical importance for auditory processing. Whilst convention maintains that FFR derives mainly from the brainstem, it has been argued recently that there are additional contributions to FFR from the auditory cortex. Using a combination of tDCS, that altered neural excitability of auditory cortices, and EEG recording, the present study provided the first evidence to validate a causal relationship between the right auditory cortex and speech-evoked FFR. The finding supports the right-asymmetric auditory cortical contributions to processing of speech periodicity and

advances our understanding of how speech signals are encoded and analysed along the central auditory pathways.

Introduction

Speech-evoked frequency-following response (FFR) is a phase-locked neural activity that reflects early processing of periodic features of input speech signals in the human brain (Picton and Aiken, 2008; Coffey et al., 2019).

The FFR is closely related to fundamental auditory processes. For instance, it plays an important role in pitch perception. FFR reflects the neural fidelity of linguistic pitch and is stronger in tonal language than non-tonal language speakers (Krishnan et al., 2004, 2005, 2009). It has greater strength in musicians who have better pitch discrimination ability than people without musical training (Musacchia et al., 2007; Wong et al., 2007; Strait et al., 2009; Bidelman et al., 2011). Furthermore, FFR is important for speech-in-noise perception. Greater FFR magnitudes are associated with better speech recognition ability in noisy environments (Song et al., 2011; Parbery-Clark et al., 2011). FFR also reflects neural plasticity related to fundamental cognitive and physiological processes such as auditory learning (Skoe et al., 2014), changes in arousal (Mai et al., 2019) and attention (Lehmann and Schönwiesner, 2014; Hartmann and Weisz, 2019).

Clinically, FFR is proposed as a biomarker for various auditory and language disorders. FFR declines with age (Anderson et al., 2012; Presacco et al., 2016) and can predict word recognition ability during speech-in-noise perception in older adults (Anderson et al., 2011; Fujihira and Shiraishi, 2015; Mai et al., 2018). This indicates that degradations to FFR could potentially explain the increased speech-in-noise difficulty experienced during aging. FFRs are also associated with hearing deficits such as cochlear synaptopathy (Encina-Llamas et al., 2019) and auditory processing disorders (Schochat et al., 2017). Furthermore, FFR is a potential marker for detecting functional impairments in learning and cognitive disorders in children, such as learning difficulties in literacy (Cunningham et al., 2001; Banai et al., 2007; White-Schwoch et al., 2015), dyslexia (Hornickel et al., 2013) and autism (Russo et al., 2008).

It is argued that the fundamental and clinical importance of FFR is linked to the neural fidelity of speech in the inferior colliculus at the brainstem, which has been proposed as the

main neural origin of FFR (Chandrasekaran and Kraus, 2010; Bidelman, 2015, 2018). Recent studies, however, have shown an additional source of FFR in the right auditory cortex associated with musical experience, pitch discrimination ability (Coffey et al., 2016), speech-in-noise perception (Coffey et al., 2017a) and intermodal attention (Hartmann and Weisz, 2019). FFR strength is associated with right-lateralized hemodynamic activity in the auditory cortex (Coffey et al., 2017b), consistent with the relative specialization of right auditory cortex for pitch and tonal processing (Zatorre and Berlin, 2001; Patterson et al., 2002; Hyde et al., 2008; Albouy et al., 2013; Cha et al., 2016).

Despite findings that show the potential cortical contribution to FFRs, it is unclear whether the relationship between auditory cortex and FFR is causal. The aim of the present study was to determine such relationship. Here, transcranial direct current stimulation (tDCS) was applied to alter neural excitability in the left and right auditory cortices. We examined the after-effects of tDCS on speech-evoked FFR using electroencephalography (EEG). tDCS is a non-invasive neuro-stimulation that modulates cortical excitability (Jacobson et al., 2012). By applying direct currents over the scalp, tDCS leads to neural excitation or inhibition in proximal parts of the cortex that last for up to 90 minutes post-stimulation (Nitsche and Paulus, 2001). Previous studies showed that applying tDCS over the right, compared to the left, auditory cortex can significantly change pitch discrimination performances, supporting the causal role of the right auditory cortex for pitch perception (Mathys et al., 2010; Matsushita et al., 2015). However, such causality has not been established for neurophysiological signatures like FFR. The present study tested the hypothesis that tDCS over the right auditory cortex should change the FFR strength during monaural listening to speech syllables. We further predicted that such after-effects should occur particularly along the contralateral auditory pathway where participants listen to speech from the left ear.

Materials and Methods

Participants

Ninety participants (18-40 years old; 45 females) were recruited and completed the entire experiment. Two other participants dropped out during the tDCS phase because they felt uncomfortable with the skin sensation when stimulation was applied. All participants had normal hearing (pure-tone audiometric thresholds <25 dB HL within frequency range of 0.25–

6 kHz for both ears) tested using a MAICO MA41 Audiometer (MAICO Diagnostics, Germany). Participants were non-tonal language speakers, had no long-term musical training and reported no history of neurological or speech/language disorders. They had not participated in any brain stimulation experiments in the two weeks prior to the present experiment.

All participants were right-handed (Handedness Index (HI) > 40; Oldfield, 1971). They were assigned at random to one of five groups, each of which received different types of tDCS (detailed in *Experimental design*). HI did not differ significantly between the five groups (all $p > 0.4$, uncorrected), indicating that the degree of handedness was well-matched across stimulation types. The absence of HI differences across groups is important because it has been argued that handedness influences functional hemispheric specialization (Carey et al., 2014; Willems et al., 2014). Hence matching the HI across groups ensured that any effects of tDCS were not confounded by handedness.

Syllable stimulus for the FFR recording

A 120-ms-long syllable /i/ spoken by a male with a static fundamental frequency (F_0) at 136 Hz was used for the FFR recordings. The waveform and spectrum of the syllable are shown as **Figure 1**. The syllable has three formants (F1, F2 and F3 at ~280, 2400 and 3100 Hz, respectively). It has a stable amplitude profile across the syllable period except for the 5-ms rising and falling cosine ramps applied at the onset and offset to avoid transients.

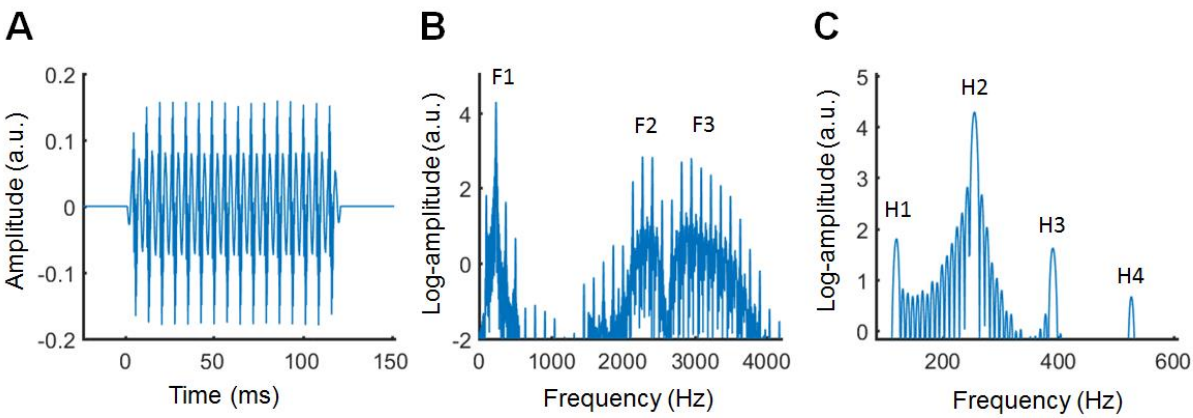

Figure 1. The syllable stimulus for FFR recordings. (A) Temporal waveform of the syllable /i/. **(B)** Spectrum of the syllable (0–4000 Hz) showing the formant locations (F1, F2 and F3). **(C)** The same spectrum as **(B)** that shows the first four harmonics with F_0 at 136 Hz. *N.B.*, the spectrum was obtained via Fast Fourier Transform (FFT) after zero-padding the temporal waveform to 1 second.

Experimental design

The experimental procedure is summarized in **Figure 2**. FFRs were recorded pre- and post-tDCS during monaural listening to the syllable stimulus to test for any after-effects of tDCS.

FFR recording

EEG were recorded over participants' scalps using an ActiveTwo system (Biosemi ActiView, The Netherlands) with sampling rate of 16,384 Hz whilst they listened to the repeatedly-presented syllable /i/ (see *Syllable stimulus for the FFR recording*) both pre- and post-tDCS. The recording site was at the vertex (Cz) localized using a standard Biosemi cap, which is the conventional site used for obtaining FFRs (Skoe and Kraus, 2010). Bilateral earlobes served as the reference and ground electrodes were CMS and DRL at the parieto-occipital sites. Electrode impedance was kept below 35 mV. The syllable stimulus was presented at ~4 times per second with inter-stimulus interval (ISI) fixed at 120 ms. The stimulus was played monaurally via electrically-shielded inserted earphone (ER-3 insert earphone, Intelligent Hearing Systems, Miami, FL) at 85 dB SL (excluding ISIs) in each ear (e.g. left-ear listening followed by right-ear listening or vice versa with order of ear presentation counterbalanced across participants). Monaural listening ensured that after-effects of ipsilateral and contralateral tDCS (relative to the listening ears) could be tested separately (see *Statistical analyses*). For each ear, there were 1,500 sweeps for the positive and 1,500 sweeps for the negative polarity presented in an intermixed order (i.e., 3,000 sweeps in total).

Participants were seated comfortably in an armchair in an electromagnetically- and sound-shielded booth. They listened passively to the stimulus sequence whilst keeping their eyes on a fixation cross in the centre of a computer screen. The 3,000 syllable sweeps in each ear were broken into six 2-minute-long blocks (500 sweeps each) with ~40 second breaks between blocks. Participants were required to keep awake and refrain from body and head movements whilst they were listening to the sounds. The FFR recording lasted for ~30 minutes for both pre- and post-tDCS. The post-tDCS recording was completed within 45 minutes post-tDCS for all participants to ensure that any after-effects of tDCS on FFRs were sustained (Nitsche and Paulus, 2001).

tDCS

tDCS was applied over the scalp using a battery-driven direct current stimulator (Magstim HDCStim, UK) with a pair of rubber-surface electrodes (5×5 cm) contained in saline-soaked cotton pads. Participants were assigned at random to one of the five groups (18 participants (9 females) per group; single-blinded). The five groups received the following different types of tDCS: (1) anodal stimulation on the left auditory cortex (AC) (Left-Anod); (2) cathodal stimulation on the left AC (Left-Cathod); (3) anodal stimulation on the right AC (Right-Anod); (4) cathodal stimulation on the right AC (Right-Cathod); and (5) Sham, with electrode configurations randomly chosen from (1)–(4) for each participant (in this group, the active electrode was put on the left AC for half of the participants and on the right AC for the other half). Centre position of the active electrode was on T7/T8 (according to the 10/20 EEG system) for the left/right AC. The reference electrode was placed on the forehead above the eyebrow contralateral to the active electrode (see Matsushita et al., 2015; also see **Figure 2**). For groups (1)–(4), tDCS was applied at 1 mA for 25 minutes with the currents ramping up/down for 15 seconds at the stimulation onset/offset. Sham applied tDCS only for 30 seconds in total (15 seconds ramping up and down respectively) at the onset of stimulation. This created the usual sensations associated with tDCS in Sham but without actual stimulation during the remainder of the run. All experimental sessions were conducted during the day time (mornings or early afternoons) and all participants had enough sleep (at least 6 hrs) the night before (based on self-report prior to the experiment) to ensure adequate cortical plasticity triggered by tDCS (Salehinejad et al., 2019).

During tDCS, participants completed a pitch discrimination task while they listened to sound stimuli over a loudspeaker 1 metre in front of them in the same sound-shielded booth used for the FFR recordings. Three short complex tones (400 ms) were presented on each trial at a calibrated level of 75 dB SL at the 1 metre position. The task was an 'ABX' task. In each trial, two tones 'A' and 'B' with different fundamental frequencies (F_0) were played consecutively followed by a third tone 'X' randomly selected from 'A' or 'B'. Participants had to identify whether 'X' was the same as 'A' or 'B'. They gave their best guess when they were unsure of the answer. The process followed a '2-down, 1-up' adaptive procedure, in which the F_0 difference between 'A' and 'B' decreased by $\sqrt{2}$ times following two consecutive correct trials and increased by $\sqrt{2}$ times following an incorrect trial. No feedback about response accuracy was provided. Half-minute breaks were taken every 4 minutes. This task was included during tDCS because tDCS preferentially modulates neural networks that are currently active (Reato et al., 2010; Ranieri et al., 2012; Bikson and Rahman, 2013).

Concurrent tDCS and the pitch discrimination task could therefore maintain auditory cortical activity during neuro-stimulation, hence maximizing the effect of tDCS on neural excitability.

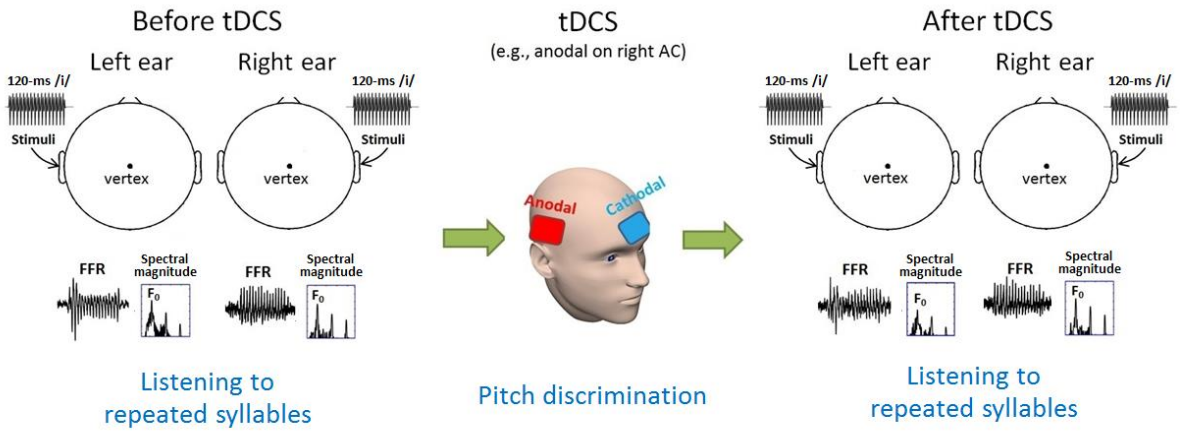

Figure 2. Illustrations for the experiment design. Participants first listened to a repeated syllable /i/ monaurally while FFR was recorded over scalp-EEGs at Cz. tDCS was then applied over the auditory cortex (AC) along with a pitch discrimination task. The same syllable listening task as in the first step was finally performed following tDCS to detect any after-effects of neuro-stimulation.

EEG Signal processing

All EEG signal processing was conducted via Matlab R2017a (The Mathworks).

Pre-processing

As mentioned, the FFR was captured from Cz. The EEG signals were first re-referenced to the bilateral earlobes and bandpass-filtered between 90 and 4000 Hz using a 2nd-order zero-phase Butterworth filter. The filtered signals were then segmented for each sweep (-50 to 150 ms relative to the syllable onset). Each segment was baseline-corrected by subtracting the average of the pre-stimulus (-50–0 ms) period. Segments that exceeded ±25 mV were rejected to minimize movement artefacts. The resultant rejection rates were < 2.5% averaged across participants for all cases (pre- and post-tDCS for the five stimulation groups for both left and right ear conditions).

FFR magnitudes

FFRs with the positive and negative polarities (FFR_{Pos} and FFR_{Neg}) were first obtained by temporally averaging the pre-processed signals across sweeps with the respective polarities. FFRs for envelopes of F_0 and its harmonics (i.e., periodicity; FFR_{ENV}) and temporal fine structures (TFS; FFR_{TFS}) were obtained by adding and subtracting FFR_{Pos} and FFR_{Neg}, respectively (Aiken and Picton, 2008). The addition and subtraction minimized the responses to TFS in FFR_{ENV} and to envelopes in FFR_{TFS}, so that purer FFRs to envelopes and TFS were obtained separately (Aiken and Picton, 2008). Spectral magnitudes of FFR_{ENV} and FFR_{TFS} were then calculated.

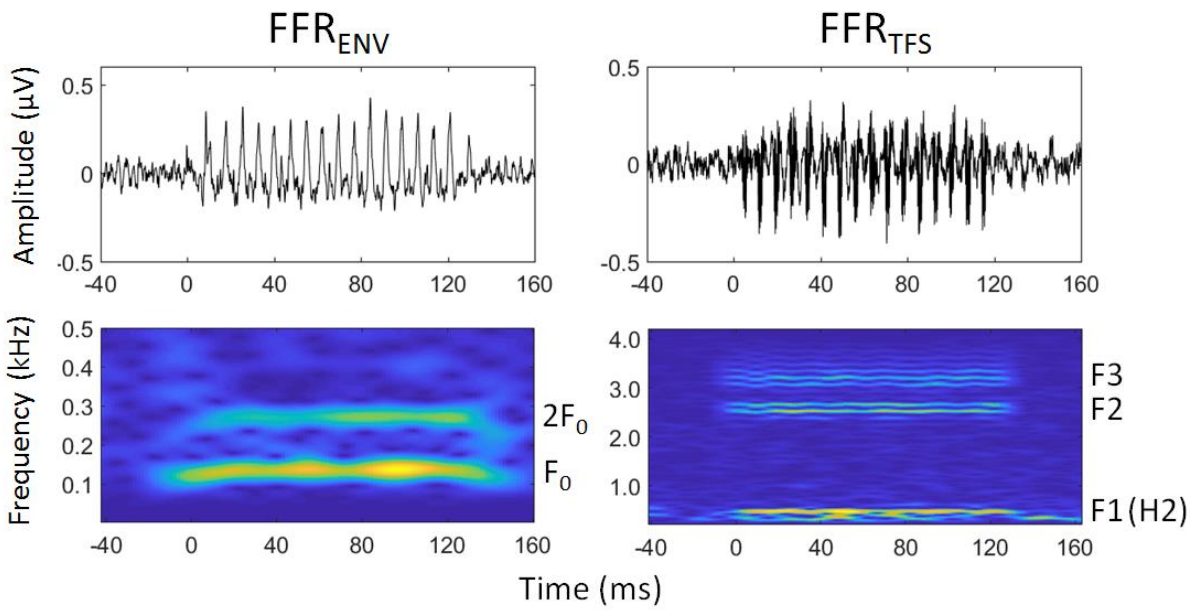

Figure 3. A representative sample of FFR. Sample waveforms (top panels) and the corresponding spectrograms (lower panels) of FFR_{ENV} (left) and FFR_{TFS} (right) were obtained from a single participant in the left ear listening condition before tDCS was applied. The first two harmonics of F_0 (F_0 and $2F_0$) dominate the power of FFR_{ENV} as indicated in the FFR_{ENV} spectrogram (lower left). The three formants (F1, F2 and F3) in FFR_{TFS} are shown and indicated in the FFR_{TFS} spectrogram (lower right); F1 occurs at H2 for this vowel (the 2nd harmonic).

For FFR_{ENV}, FFR_{ENV_F0} and FFR_{ENV_2F0} (FFR_{ENV} at F_0 and its 2nd harmonic, $2F_0$) that dominate the power of FFR_{ENV} (see **Figure 3** left panel) were focused on. Whereas FFR_{ENV_F0} and FFR_{ENV_2F0} reflect neural phase-locking to the stimulus envelope periodicity in the central auditory systems, higher harmonics (≥ 3) of FFR_{ENV} may reflect distortion products resulting from non-linearities in response to acoustic stimuli on the basilar membrane (Smalt et al.,

2012). Whilst it is expected that FFR_{ENV_F0} plays the major role in phase-locking to speech periodicity, FFR_{ENV_2F0} also makes contributions (e.g., Aiken and Picton, 2008) because of the non-sinusoidal characteristics of speech periodicity (Holmberg et al., 1988; also see discussions in Smalt et al., 2012). The procedure for measuring the magnitudes of FFR_{ENV_F0} and FFR_{ENV_2F0} was as follows: a set of 120 ms (same length as the stimulus syllable) sliding windows (1 ms per step), each with a 5-ms rising/falling cosine ramp at the onset/offset, was applied to the FFR_{ENV} waveform. As FFR_{ENV} occurs at the auditory brainstem (Chandrasekaran and Kraus, 2010; Bidelman, 2015, 2018) and/or primary auditory cortex (Coffey et al., 2016), the neural transmission delays were set at 5–20 ms. Onsets of the windows were therefore set at 6–21 ms (allowing for an additional ~1 ms sound transmission through the plastic tube of the earphone to the cochlea) after the syllable onset. The windowed FFR_{ENV} waveform in each step was then zero-padded to 1 second to allow for a frequency resolution of 1 Hz and the log-transformed FFT-powers ($10*\log_{10}$[power]) centred at F_0 and $2F_0$ were measured (averaged across 136 ± 2 Hz and 272 ± 2 Hz, respectively). Finally, the FFR_{ENV_F0} and FFR_{ENV_2F0} magnitudes were taken as the powers at the optimal neural delays (i.e., when powers are maximal across all steps for F_0 and $2F_0$, respectively).

For FFR_{TFS}, FFR_{TFS_H2} and FFR_{TFS_F2F3} (FFR_{TFS} at the 2nd harmonic that represents F1 for this vowel, and at F2 and F3, respectively; see **Figure 4.3** right panel) were focused on. FFR_{TFS_H2} reflects FFR to TFS at the resolved-harmonic region while FFR_{TFS_F2F3} reflects FFR to TFS at the unresolved-harmonic region. The same procedure used when measuring magnitudes of FFR_{ENV_F0} and FFR_{ENV_2F0} was followed, except that: (1) the procedure was applied on FFR_{TFS} at H2 (for FFR_{TFS_H2}) and at H16–H27 (the 16th to 27th harmonics corresponding to the range of F2 and F3 for FFR_{TFS_F2F3}; the final magnitude was taken as the mean magnitude across all harmonics in this range); (2) the neural delays during analyses were set at 1–6 ms (0–5 ms delays allowing an additional 1 ms sound transmission through the plastic tube of the earphone) as FFR_{TFS} arises at earlier stages of auditory processing in the periphery (Aiken and Picton, 2008).

Because of the different neural origins of FFR_{ENV} (brainstem/auditory cortex) and FFR_{TFS} (periphery), the present study thus allows us to confirm whether tDCS applied to auditory cortex affects FFR that arise at different levels of the auditory systems.

Statistical analyses

Before testing the after-effects of tDCS, analyses were first conducted to check whether baseline (pre-tDCS) characteristics were matched across stimulation. ANOVAs were conducted using the baseline magnitudes and optimal neural delays of FFRs as dependent variables, Stimulation (Left-Anod, Left-Cathod, Right-Anod, Right-Cathod and Sham) and Ear (left vs. right) as independent variables. Post-hoc analyses were conducted following significant interactions or main effects.

After-effects of tDCS (differences in FFR magnitudes between post- and pre-tDCS) were tested using linear mixed-effect regressions. These were conducted using after-effects as dependent variables, Stimulation and Ear as fixed-effect factors and Participant as the random-effect factor. Post-hoc analyses were conducted following significant interactions or main effects.

Furthermore, regardless of whether interaction effects occurred between Stimulation and Ear, planned comparisons for the after-effects were conducted between different stimulation types in the left and right ear conditions, respectively. This was because collapsing the left and right ears would smear the distinctions between any after-effects along the contralateral pathway (ears with tDCS on the opposite side) and those along the ipsilateral pathway (ears with tDCS on the same side), which was one of the aspects addressed in the present study. As multiple comparisons were conducted for each ear (5 stimulation types leading to 10 comparisons), the critical α value for detecting significance was adjusted at 0.005. It was predicted that, compared to Sham, significantly greater after-effects of tDCS over the right auditory cortex (Right-Anod and Right-Cathod), but not the left auditory cortex (Left-Anod or Left-Cathod), should be found, consistent with the current hypothesis that the right auditory cortex makes specific contributions to FFR.

FFR magnitudes were magnitudes of FFR_{ENV} (FFR_{ENV_F0} and FFR_{ENV_2F0}) and FFR_{TFS} (FFR_{TFS_H2} and FFR_{TFS_F2F3}) (see *EEG signal processing*). For FFR_{ENV}, the present study combined the magnitudes of FFR_{ENV_F0} and FFR_{ENV_2F0}, rather than use them as separate dependent variables. The reason was that, it was observed that the summed FFR_{ENV_F0} and FFR_{ENV_2F0} magnitude yielded greater effect sizes during planned comparisons where statistical significance ($p < 0.05$, uncorrected) was detected using FFR_{ENV_F0} or FFR_{ENV_2F0} magnitude alone: Cohen's d = 0.752 and 1.001 for FFR_{ENV_F0} and for the summed FFR_{ENV_F0} and FFR_{ENV_2F0} magnitude, respectively, when Right-Anod was compared with Sham in the left ear listening condition; Cohen's d = 0.934 and 1.140 for FFR_{ENV_F0} and for combined FFR_{ENV_F0}

and FFR_{ENV_2F0} magnitude, respectively, when Right-Cathod was compared with Sham in the left ear listening condition (see *Results* for further details).

Results

Baseline characteristics

Table 1 and **2** shows the baseline magnitudes and neural delays for FFR_{ENV}, FFR_{TFS_H2} and FFR_{TFS_F2F3} in both the left and right ear conditions. ANOVAs were conducted for baseline magnitudes and optimal neural delays of FFR_{ENV}, FFR_{TFS_H2} and FFR_{TFS_F2F3}.

For FFR_{ENV}, a significant main effect of Ear was found for the magnitude ($F(1, 85) = 12.318$, $p < 0.001$; greater magnitude in the left than in the right ear condition) but not for the neural delay ($F(1, 85) = 0.055$, $p = 0.815$); no main effects of Stimulation (magnitude: $F(4, 85) = 0.932$, $p = 0.450$; neural delay: $F(4, 85) = 0.799$, $p = 0.529$) or [Stimulation × Ear] interactions were found (magnitude: $F(4, 85) = 0.541$, $p = 0.706$; neural delay: $F(4, 85) = 0.046$, $p = 0.996$). Furthermore, no significant differences were found between any stimulation type in either ear condition (magnitude: all $p > 0.07$; neural delay: all $p > 0.1$). **Figure 4** illustrates the comparison of baseline magnitudes for FFR_{ENV} between the left and right ear conditions after collapsing across stimulation types (due to the significant main effect of Ear but no main effect of Stimulation).

For FFR_{TFS_H2}, there were no significant main effects of Stimulation (magnitude: $F(4, 85) = 0.692$, $p = 0.600$; neural delay: $F(4, 85) = 1.421$, $p = 0.234$) or Ear (magnitude: $F(1, 85) = 3.483$, $p = 0.065$; neural delay: $F(1, 85) = 1.842$, $p = 0.178$), or [Stimulation × Ear] interactions (magnitude: $F(4, 85) = 0.744$, $p = 0.565$; neural delay: $F(4, 85) = 0.587$, $p = 0.673$). No significant differences were found between any stimulation type in either ear condition (magnitude: all $p > 0.1$; neural delay: all $p > 0.05$).

For FFR_{TFS_F2F3}, significant main effects of Stimulation ($F(4, 85) = 40.872$, $p < 0.001$) and Ear ($F(1, 85) = 4.225$, $p = 0.002$; greater in the right than the left ear condition) were found for the magnitude, but not for the neural delay (Stimulation: $F(4, 85) = 1.504$; $p = 0.208$; Ear: $F(1, 85) = 0.324$, $p = 0.571$). A significant [Stimulation × Ear] interaction was found for the neural delay ($F(4, 85) = 2.549$, $p = 0.045$), but not for the magnitude ($F(4, 85) = 1.763$, $p =$

0.144). Post-hoc analyses found significant differences in magnitudes between several stimulation types (collapsing the left and right ears: Left-Anod vs. Right-Anod, t(34) = -2.110, p = 0.042; Left-Anod vs. Sham, t(34) = -2.713, p = 0.010; Left-Cathod vs. Right-Anod, t(34) = -2.796, p = 0.008; Left-Cathod vs. Right-Cathod, t(34) = -2.566, p = 0.015; Left-Cathod vs. Sham, t(34) = -3.498, p = 0.001). Significant differences were found between stimulation types for the neural delay in both the left ear (Left-Anod vs. Right-Cathod, t(34) = -2.703, p = 0.011) and the right ear condition (Right-Anod vs. Right-Cathod, t(34) = 2.279, p = 0.029; Left-Anod vs. Right-Anod, t(34) = -2.240, p = 0.032; Right-Anod vs. Sham, t(34) = 2.629, p = 0.013). All p-values here are reported without correction.

The results thus indicate that the baseline characteristics of FFR_{ENV} and FFR_{TFS_H2}, but not FFR_{TFS_F2F3}, were well matched across stimulation types. As such, although after-effects were tested for all three FFR signatures, FFR_{ENV} and FFR_{TFS_H2} are focused on. In addition, the main effects of Ear for FFR_{ENV} and FFR_{TFS_F2F3} magnitudes may reflect the laterality of speech encoding at the subcortical (Chandrasekaran and Kraus, 2010; Bidelman, 2015, 2018) and/or cortical levels (Coffey et al., 2016, 2017b), which will be discussed further (see *Discussion*).

Table 1. Baseline magnitudes (standard deviations shown in the brackets; in *dB*) for FFR_{ENV}, FFR_{TFS_H2} and FFR_{TFS_F2F3} across stimulation types in the left and right ear conditions.

FFRs	Ear	Left-Anod	Left-Cathod	Right-Anod	Right-Cathod	Sham
FFR_{ENV}	Left	76.28 (5.27)	78.84 (7.03)	76.05 (6.96)	76.24 (8.56)	73.45 (10.05)
	Right	75.05 (5.79)	75.42 (4.72)	72.82 (6.62)	74.24 (7.91)	72.17 (10.92)
FFR_{TFS_H2}	Left	30.35 (5.70)	30.70 (7.71)	32.52 (7.12)	31.68 (6.24)	33.37 (6.86)
	Right	32.71 (3.88)	30.63 (6.98)	32.59 (7.97)	33.40 (7.51)	34.36 (5.66)
FFR_{TFS_F2F3}	Left	15.31 (7.26)	13.21 (7.24)	19.45 (7.16)	20.14 (6.58)	20.46 (5.75)
	Right	17.13 (7.07)	16.28 (6.58)	22.97 (7.57)	20.90 (7.82)	23.58 (6.09)

Table 2. Baseline neural delays (standard deviations shown in the brackets; in *ms*) for FFR_{ENV}, FFR_{TFS_H2} and FFR_{TFS_F2F3} across stimulation types in the left and right ear conditions.

FFRs	Ear	Left-Anod	Left-Cathod	Right-Anod	Right-Cathod	Sham
FFR_{ENV}	Left	8.75 (2.45)	9.42 (2.44)	9.67 (2.70)	8.56 (2.81)	8.81 (2.71)
	Right	8.78 (2.02)	9.47 (3.49)	9.50 (3.25)	8.58 (1.69)	9.08 (2.33)
FFR_{TFS_H2}	Left	3.50 (2.28)	4.50 (1.82)	3.50 (1.82)	3.67 (2.06)	4.28 (1.60)
	Right	3.61 (2.30)	4.94 (1.59)	4.44 (1.95)	4.11(2.00)	4.06 (1.92)
FFR_{TFS_F2F3}	Left	2.90 (0.36)	3.04 (0.27)	3.03 (0.44)	3.20 (0.31)	3.05 (0.53)
	Right	2.93 (0.48)	3.03 (0.48)	3.28 (0.47)	2.97 (0.34)	2.87 (0.48)

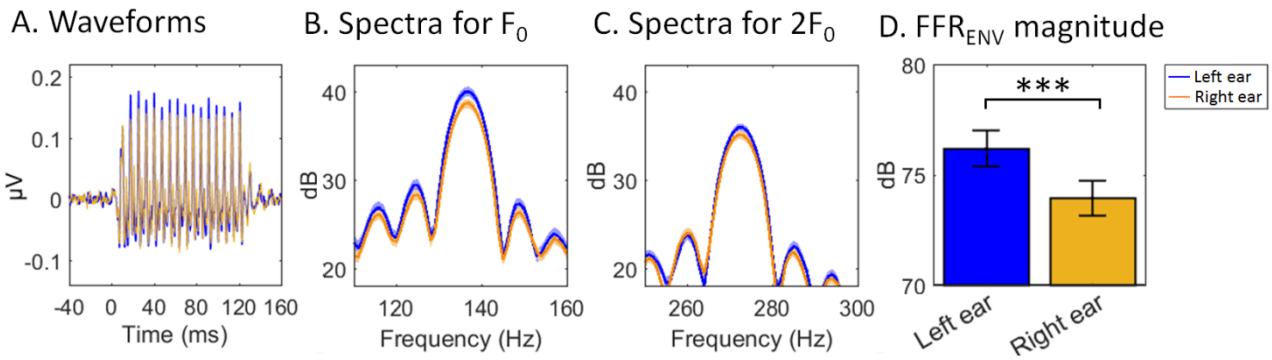

Figure 4. Comparison of baseline magnitude for FFR_{ENV} between the left and the right ear conditions. The comparison was conducted by collapsing the stimulation types following the ANOVA results which showed a significant main effect of Ear, but no significant main effect of Stimulation or [Stimulation × Ear] interaction for the baseline FFR_{ENV} magnitude. The left and the right ear conditions are indicated as *blue* and *orange*, respectively. **(A)** Waveforms of FFR_{ENV} averaged across stimulation types. **(B)(C)** FFT-power spectra averaged across stimulation types, obtained using the individual optimal neural delays for **(B)** FFR_{ENV_F0} (showing 110–160 Hz peaking at F_0 of 136 Hz) and **(C)** FFR_{ENV_2F0} (showing 250–300 Hz peaking at $2F_0$ 272 Hz) (shaded areas in the spectra cover the ranges of ±1 standard errors (SEs)). **(D)** FFR_{ENV} magnitude (summed magnitude of FFR_{ENV_F0} and FFR_{ENV_2F0}). Significant greater FFR_{ENV} magnitude was found in the left than in the right ear condition (***$p < 0.001$, uncorrected). Error bars indicate the SEs.

After-effects on FFR_{ENV}

FFR_{ENV} magnitude refers to the summed FFR_{ENV_F0} and FFR_{ENV_2F0} magnitudes (see Statistical analyses). **Figure 5** shows the waveforms and FFT-power spectra for FFR_{ENV} across

participants. Linear mixed-effect regression showed a significant main effect of Stimulation ($F(4, 85) = 2.549$, $p = 0.045$). No main effect of Ear ($F(1, 85) = 0.784$, $p = 0.378$) or [Stimulation × Ear] interaction ($F(4, 85) = 1.309$, $p = 0.273$) was found. Post-hoc independent-sample t-tests were thus conducted between different stimulation types following the main effect of Stimulation (collapsing the left and right ear due to the lack of [Stimulation × Ear] interaction). After-effects of tDCS over the right AC were significantly lower than that of Sham (Right-Anod vs. Sham, $t(34) = -2.569$, $p = 0.015$ (uncorrected), Cohen's $d = 0.856$; Right-Cathod vs. Sham, $t(34) = -2.219$, $p = 0.033$ (uncorrected), Cohen's $d = 0.740$) (**Figure 6**).

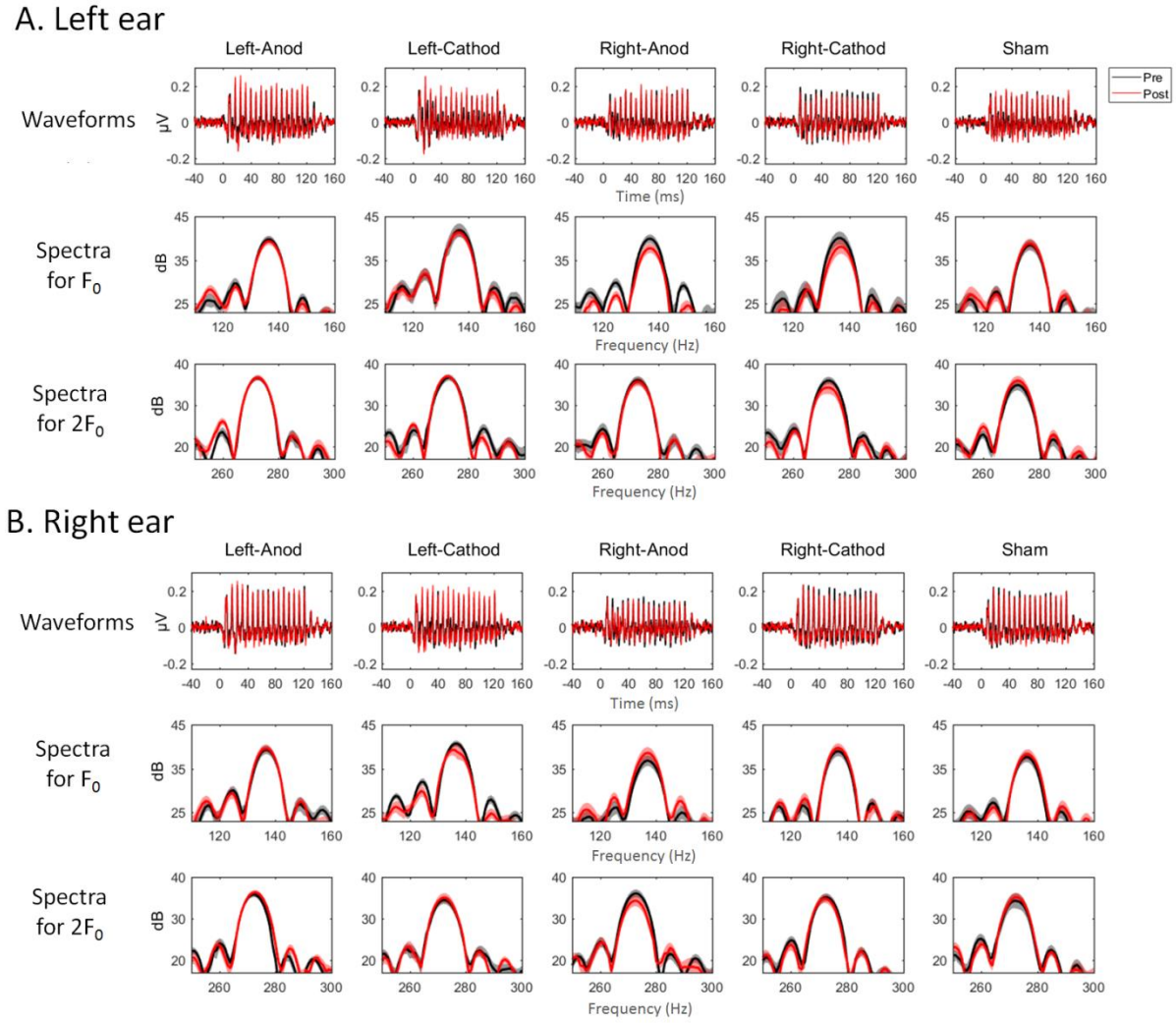

Figure 5. Waveforms and power spectra for FFR_{ENV} averaged across participants. **(A)** and **(B)** show the waveforms and FFT-power spectra in the left and right ear condition, respectively. Pre- and post-tDCS were indicated as *black* and *red*, respectively (shaded areas in the spectra cover the ranges of ±1 SEs from the means). From left to right are different

stimulation types (Left-Anod, Left-Cathod, Right-Anod, Right-Cathod and Sham). *Upper* panels: waveforms of FFR_{ENV}; *mid* and *lower* panels: power spectra obtained using the individual optimal neural delays for FFR_{ENV_F0} (*mid*; showing 110–160 Hz peaking at F_0 of 136 Hz) and FFR_{ENV_2F0} (*lower*; showing 250–300 Hz peaking at $2F_0$ of 272 Hz).

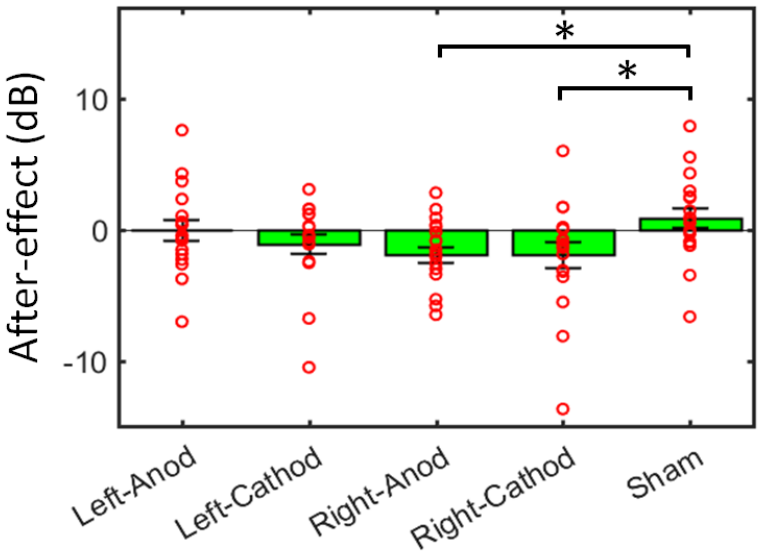

Figure 6. After-effects of tDCS on FFR_{ENV} magnitudes comparing across stimulation types after collapsing the left and right ears. Collapsing the left and right ears was conducted following the ANOVA results which showed a significant main effect of Stimulation but no significant main effect of Ear or [Stimulation × Ear] interaction. Red circles indicate individual data for the corresponding stimulation types (Left-Anod, Left-Cathod, Right-Anod, Right-Cathod and Sham). Post-hoc paired comparisons showed significant differences between tDCS over the right AC (Right-Anod and Right-Cathod) and Sham (*p < 0.05, uncorrected). Error bars indicate the SEs.

Planned comparisons between different stimulation types were subsequently conducted for the left and right ear listening conditions to determine whether tDCS has effects along the contralateral or ipsilateral pathway. The critical α value for detecting significance was adjusted to 0.005 (there were 10 pairs of comparisons in each ear condition). The results are illustrated in **Figure 7** (upper panels). In the left ear condition, significant differences were found between tDCS over the right AC and Sham (Right-Anod vs. Sham, $t(34) = -3.024$, $p < 0.005$, Cohen's *d*

= 1.001; Right-Cathod vs. Sham, t(34) = -3.420, p = 0.002, Cohen's d = 1.140). No significant effects were found for any other comparison (all p > 0.2). In the right ear condition, no significant effects were found for any pair of comparison (all p > 0.2). All p-values shown here are reported without correction.

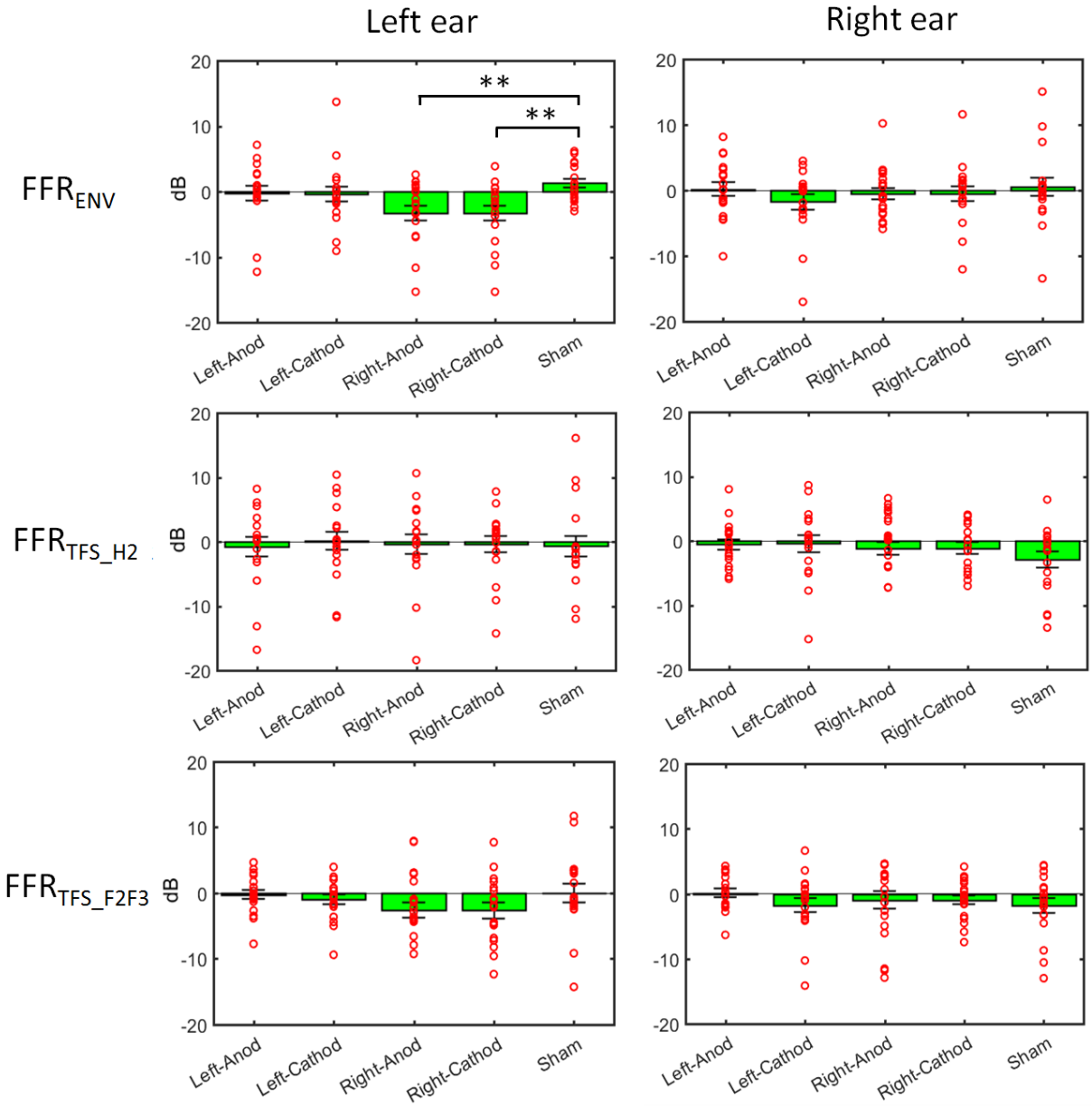

Figure 7. After-effects of tDCS on FFR magnitudes. Upper, mid and lower panels indicate the after-effects on magnitudes of FFR_{ENV}, FFR_{TFS_H2} and FFR_{TFS_F2F3}, respectively. Planned comparisons were conducted between different stimulation types in both the left and right ear conditions, with the critical α value set at 0.005 according to multiple comparisons. Significant differences were found between tDCS over the right auditory cortex (Right-Anod and Right-Cathod) and Sham in the left ear condition for FFR_{ENV}. (**p < 0.005, uncorrected; i.e., p <

0.05 after correction according to multiple comparisons) Red circles indicate individual data for the corresponding stimulation types. Error bars indicate the SEs.

After-effects on FFR_{TFS}

Equivalent analyses to those conducted for the FFR_{ENV} magnitude were conducted for the magnitudes of FFR_{TFS_H2} and FFR_{TFS_F2F3}. The linear mixed-effect regressions did not show significant main effects of Stimulation (FFR_{TFS_H2}: $F(4, 85) = 0.528$, $p = 0.715$; FFR_{TFS_F2F3}: $F(4, 85) = 0.613$, $p = 0.655$) or Ear (FFR_{TFS_H2}: $F(1, 85) = 0.496$, $p = 0.467$; FFR_{TFS_F2F3}: $F(1, 85) = 0.213$, $p = 0.646$), or significant [Stimulation × Ear] interactions (FFR_{TFS_H2}: $F(4, 85) = 0.530$, $p = 0.714$; FFR_{TFS_F2F3}: $F(4, 85) = 1.189$, $p = 0.322$).

Planned comparisons did not find significant after-effects between different stimulation types in the left or right ear condition (FFR_{TFS_H2}: all $p > 0.6$ in the left ear condition and all $p > 0.1$ in the right ear condition; FFR_{TFS_F2F3}: all $p > 0.09$ in the left ear condition and all $p > 0.1$ in the right ear condition; see **Figure 7**, mid and lower panels). All *p*-values are reported without correction.

Discussion

The current study used a combined tDCS and EEG approach to test for a causal contribution of auditory cortex to speech-evoked FFR in healthy right-handed participants. The left and right auditory cortices were neuro-stimulated in different groups of participants and the after-effects of tDCS on the FFR were examined during monaural listening to a repeated speech syllable. The results showed that tDCS, both anodal and cathodal, over the right auditory cortex, generated significantly greater after-effects on FFR_{ENV} magnitude compared to sham stimulation. Specifically, such effects were present only in the left ear listening condition, indicating that the changes in processing of speech periodicity information occur along the contralateral pathway (i.e., from the left ear to the right auditory cortex). The results thus agree with previous studies that have shown a close relation between the right auditory cortex and FFR (Coffey et al., 2016, 2017a, 2017b; Hartmann and Weisz, 2019) and provide the first evidence for a causal relationship.

Laterality for FFR_{ENV} at the baseline

Ear laterality for the baseline FFR_{ENV} and FFR_{TFS_F2F3} magnitudes were found (see *Baseline characteristics*). The discussion here focuses on FFR_{ENV} alone due to the significant main effect of Stimulation for the baseline FFR_{TFS_F2F3} magnitude (which means that the baseline was not well matched across stimulation types) and lack of a significant after-effect of tDCS on FFR_{TFS_F2F3} magnitude.

The present study found that baseline FFR_{ENV} had significantly greater magnitude in the left than in the right ear condition, supporting the lateralization of speech periodicity encoding along the contralateral auditory pathway from the left ear to the right auditory cortex. This echoes the previous findings that showed the right-hemispheric lateralization of the classic 40 Hz auditory steady-state response (ASSR) (Ross et al., 2005; Luke et al., 2017). Right lateralization was also found in ASSR at 80 Hz (Vanvooren et al., 2014). ASSRs are phase-locked responses to amplitude-modulated tones/noise and both ASSRs and FFR_{ENV} are envelope-following responses (Dimitrijevic et al., 2004). Whilst the 40 Hz ASSR has its main generator at the cortical level (Herdman et al., 2002; Ross et al., 2002, 2005), prominent activities occur at the brainstem level for the 80 Hz ASSR (Herdman et al., 2002) and speech-evoked FFR_{ENV} (Chandrasekaran and Kraus, 2010; Bidelman, 2015, 2018; this can also be seen in the present study where average optimal neural delays were between 5 and 10 ms, see **Table 2**). Recent studies, however, have shown that FFR has additional sources in the auditory cortex (Coffey et al., 2016, 2017a; Hartmann and Weisz, 2019). It is thus not clear whether the observed laterality of FFR_{ENV} in the present study occurs at the subcortical or cortical level or, more equivocally, whether auditory cortex contributes to this laterality. As such, the current combined tDCS and EEG approach showed how altering neural excitability of auditory cortex in the left or right hemisphere can lead to changes in FFR which therefore provides confirmatory evidence for a causal cortical contribution.

Causal role of the right auditory cortex for FFR_{ENV}

After-effects found for FFR_{ENV} but not FFR_{TFS} indicate that tDCS had impacts on the responses at the subcortical and/or cortical levels above the auditory periphery. The findings thus argue for a causal role of the right auditory cortex in processing speech periodicity information along the contralateral pathway in the central auditory systems.

The present study thus advances our understanding of the relationship between FFR and pitch processing in the right auditory cortex. Previous studies have shown that FFR is closely related to pitch perception. FFR strength can be enhanced by both short-term perceptual training of pitch discrimination (Carcagno and Plack, 2011) as well as long-term musical experience (Musacchia et al., 2007; Wong et al., 2007; Strait et al., 2009; Bidelman et al., 2011). Furthermore, FFR has been used as an index of neural fidelity of linguistic pitch and the fidelity is greater in tonal language than in non-tonal language speakers (Krishnan et al., 2004, 2005, 2009). Despite this, however, rather than reflecting the result of pitch extraction, FFR has been suggested to reflect subcortical responses to monaural temporal information (e.g., periodicity cues) that are important for extracting pitch of complex sounds (i.e., 'pitch-bearing' information; Gockel et al., 2011). On the other hand, the process of pitch extraction itself takes place in the auditory cortex (Penagos et al., 2004; Bendor and Wang, 2005; Puschmann et al., 2010) with a right hemispheric specialization (Zatorre and Berlin, 2001; Patterson et al., 2002; Hyde et al., 2008; Mathys et al., 2010; Albouy et al., 2013). In this respect, the current after-effects of tDCS may reflect a top-down corticofugal modulation process in which the right auditory cortex affects the processing of pitch-bearing information that occurs at the subcortical level. Alternatively, although EEG mainly captures FFR signals originating from the brainstem (Bidelman, 2015, 2018), cortical sources have been found dominated in the right hemisphere (Coffey et al., 2016; 2017a). It therefore cannot be excluded that tDCS may affect the FFR magnitude directly at the cortical level. It is noteworthy that the current finding could not disentangle whether the effects emerge at the subcortical or cortical level, or both.

Also, stronger evidence would be provided for the specific contributions of the right auditory cortex to FFR if significant differences in after-effects were further found between tDCS over the right and the left auditory cortex. However, the present results did not show such differences. A possible explanation is that tDCS not only alters excitability of regions in which electrodes are located but can yield widespread changes across the brain (see a review: Filmer et al., 2014). This could be due to the diffuse nature of the tDCS where currents do not only flow between electrodes, but also spread widely through various other regions (Faria et al., 2011; Bai et al., 2014; Unal and Bikson, 2018). tDCS also changes functional connectivity (Sehm et al., 2012; Kunze et al., 2016) by which interactions of auditory cortices between the two hemispheres may be further activated. Therefore, tDCS over the left auditory cortex could also cause some changes in the right side that yield similar (but smaller) after-effects as direct stimulation over the right auditory cortex.

Neurophysiological consequences of tDCS

An intriguing finding of the present study is that anodal and cathodal tDCS over the right auditory cortex resulted in the same direction of changes, both causing decreases in FFR_{ENV} magnitude compared to sham. Conventionally, anodal and cathodal stimulations reflect depolarization and hyperpolarization of neurons, respectively, which should lead to opposite directions of after-effects (Jacobson et al., 2012). However, it is not unusual that tDCS has polarity-independent effects due to the underlying complexity of its neurophysiological consequences. For example, several studies have shown that anodal and cathodal tDCS have the same effects on excitability of motor cortex (Antal et al., 2007), motor learning (de Xivry et al., 2011), cerebellar functions for working memory (Ferrucci et al., 2008) and visuomotor learning (Shah et al., 2013). The first possible explanation would be the non-linear effects of tDCS depending on the current density. It has been shown that cathodal tDCS with an electrode size of 35 cm^2 can lead to inhibition in the motor cortex at 1 mA but excitation at 2 mA (Batsikadze et al., 2013). The present study used a current intensity at 1 mA but with smaller electrode size (25 cm^2; hence greater current density). It could be that this current density through the auditory cortex would lead to non-linear effects as resulted in the motor cortex. Second, it is possible that similar changes in concentrations of relevant neurotransmitters are caused by anodal and cathodal tDCS. It was found that with 1 mA currents, anodal tDCS causes decreases in GABA concentration that lead to cortical excitation; cathodal tDCS also causes decreases in GABA, but with greater concurrent decreases in glutamate that lead to cortical inhibition (Stagg et al., 2009). It is possible that GABA concentrations, which decrease following both anodal and cathodal tDCS, play an important role for changes in FFR_{ENV} magnitude.

Conclusion

The current results validate the previous findings that the right auditory cortex makes significant contributions to speech-evoked FFR (Coffey et al., 2016, 2017a, 2017b; Hartmann and Weisz, 2019) by establishing a causal relationship between the two. To our knowledge, this is the first evidence for this causality and it could be essential due to the fundamental and clinical importance of the FFR. Thus, these findings should advance our understanding of how speech periodicity and pitch information are processed along the central auditory pathways in the human brain. Future research is needed to further clarify where exactly this causality emerges, i.e., to disentangle whether the effects are realized through top-down corticofugal

modulations on the subcortical level, or modulations directly in the cortex. Moreover, it will be worthwhile to further investigate how changes in concentrations of neurotransmitters by neuro-stimulation relate to this causality, which can help us better understand the underlying mechanisms of the cortical contributions to FFR.

References

Aiken SJ, Picton TW (2008) Envelope and spectral frequency-following responses to vowel sounds. Hearing Research 245:35-47.

Albouy P, Mattout J, Bouet R, Maby E, Sanchez G, Aguera PE, Daligault S, Delpuech C, Bertrand O, Caclin A, Tillmann B (2013) Impaired pitch perception and memory in congenital amusia: the deficit starts in the auditory cortex. Brain 136(5):1639-1661.

Anderson S, Parbery-Clark A, Yi HG, Kraus N (2011) A neural basis of speech-in-noise perception in older adults. Ear and Hearing 32(6):750.

Anderson S, Parbery-Clark A, White-Schwoch T, Kraus N (2012) Aging affects neural precision of speech encoding. Journal of Neuroscience 32(41):14156-14164.

Antal A, Terney D, Poreisz C, Paulus W (2007) Towards unravelling task‐related modulations of neuroplastic changes induced in the human motor cortex. European Journal of Neuroscience 26(9):2687-2691.

Bai S, Dokos S, Ho KA, Loo C (2014) A computational modelling study of transcranial direct current stimulation montages used in depression. NeuroImage 87:332-344.

Banai K, Abrams D, Kraus N (2007) Sensory-based learning disability: Insights from brainstem processing of speech sounds. International Journal of Audiology 46(9):524-532.

Batsikadze G, Moliadze V, Paulus W, Kuo MF, Nitsche MA (2013) Partially non‐linear stimulation intensity‐dependent effects of direct current stimulation on motor cortex excitability in humans. The Journal of Physiology 591(7):1987-2000.

Bendor D, Wang X (2005) The neuronal representation of pitch in primate auditory cortex. Nature 436(7054):1161-1165.

Bidelman GM, Krishnan A, Gandour JT (2011) Enhanced brainstem encoding predicts musicians' perceptual advantages with pitch. European Journal of Neuroscience 33(3):530-538.

Bidelman GM (2015) Multichannel recordings of the human brainstem frequency-following response: scalp topography, source generators, and distinctions from the transient ABR. Hearing Research 323:68-80.

Bidelman GM (2018) Subcortical sources dominate the neuroelectric auditory frequency-following response to speech. NeuroImage 175:56-69.

Bikson M, Rahman A (2013) Origins of specificity during tDCS: anatomical, activity-selective, and input-bias mechanisms. Frontiers in Human Neuroscience 7:688.

Carcagno S, Plack CJ (2011) Subcortical plasticity following perceptual learning in a pitch discrimination task. Journal of the Association for Research in Otolaryngology 12(1):89-100.

Carey DP, Johnstone LT (2014) Quantifying cerebral asymmetries for language in dextrals and adextrals with random-effects meta analysis. Frontiers in Psychology 5:1128.

Cha K, Zatorre RJ, Schönwiesner M (2016) Frequency selectivity of voxel-by-voxel functional connectivity in human auditory cortex. Cerebral Cortex 26(1):211-224.

Chandrasekaran B, Kraus N (2010) The scalp-recorded brainstem response to speech: Neural origins and plasticity. Psychophysiology 47(2):236-246.

Coffey EB, Herholz SC, Chepesiuk AM, Baillet S, Zatorre RJ (2016) Cortical contributions to the auditory frequency-following response revealed by MEG. Nature Communications 7(1):1-11.

Coffey EB, Musacchia G, Zatorre RJ (2017a) Cortical correlates of the auditory frequency-following and onset responses: EEG and fMRI evidence. Journal of Neuroscience 37(4):830-838.

Coffey EB, Chepesiuk AM, Herholz SC, Baillet S, Zatorre RJ (2017b) Neural correlates of early sound encoding and their relationship to speech-in-noise perception. Frontiers in Neuroscience 11:479.

Coffey EB, Nicol T, White-Schwoch T, Chandrasekaran B, Krizman J, Skoe E, Zotorre RJ, Kraus N (2019) Evolving perspectives on the sources of the frequency-following response. Nature Communications 10(1):1-10.

Cunningham J, Nicol T, Zecker SG, Bradlow A, Kraus N (2001) Neurobiologic responses to speech in noise in children with learning problems: deficits and strategies for improvement. Clinical Neurophysiology 112(5):758-767.

de Xivry JJ, Marko MK, Pekny SE, Pastor D, Izawa J, Celnik P, Shadmehr R (2011) Stimulation of the human motor cortex alters generalization patterns of motor learning. Journal of Neuroscience 31(19):7102-7110.

Dimitrijevic A, John MS, Picton TW (2004) Auditory steady-state responses and word recognition scores in normal-hearing and hearing-impaired adults. Ear and Hearing 25(1):68-84.

Encina-Llamas G, Harte JM, Dau T, Shinn-Cunningham B, Epp B (2019) Investigating the effect of cochlear synaptopathy on envelope following responses using a model of the auditory nerve. Journal of the Association for Research in Otolaryngology 20(4):363-382.

Faria P, Hallett M, Miranda PC (2011) A finite element analysis of the effect of electrode area and inter-electrode distance on the spatial distribution of the current density in tDCS. Journal of Neural Engineering, 8(6):066017.

Ferrucci R, Marceglia S, Vergari M, Cogiamanian F, Mrakic-Sposta S, Mameli F, Zago S, Babieri S, Priori A (2008) Cerebellar transcranial direct current stimulation impairs the practice-dependent proficiency increase in working memory. Journal of Cognitive Neuroscience 20(9), 1687-1697.

Filmer HL, Dux PE, Mattingley JB (2014) Applications of transcranial direct current stimulation for understanding brain function. Trends in Neurosciences 37(12):742-753.

Fujihira H, Shiraishi K. (2015). Correlations between word intelligibility under reverberation and speech auditory brainstem responses in elderly listeners. Clinical Neurophysiology, 126(1), 96-102.

Gockel HE, Carlyon RP, Mehta A, Plack CJ (2011) The frequency following response (FFR) may reflect pitch-bearing information but is not a direct representation of pitch. Journal of the Association for Research in Otolaryngology 12(6):767-782.

Hartmann T, Weisz N (2019) Auditory cortical generators of the Frequency Following Response are modulated by intermodal attention. NeuroImage 203:116185.

Herdman AT, Lins O, Van Roon P, Stapells DR, Scherg M, Picton TW (2002) Intracerebral sources of human auditory steady-state responses. Brain Topography 15(2):69-86.

Holmberg EB, Hillman RE, Perkell JS (1988) Glottal airflow and transglottal air pressure measurements for male and female speakers in soft, normal, and loud voice. The Journal of the Acoustical Society of America 84(2):511-529.

Hornickel J, Kraus N (2013) Unstable representation of sound: a biological marker of dyslexia. Journal of Neuroscience 33(8):3500-3504.

Hyde KL, Peretz I, Zatorre RJ (2008) Evidence for the role of the right auditory cortex in fine pitch resolution. Neuropsychologia 46(2):632-639.

Jacobson L, Koslowsky M, Lavidor M (2012) tDCS polarity effects in motor and cognitive domains: a meta-analytical review. Experimental Brain Research 216(1):1-10.

Krishnan A, Xu Y, Gandour JT, Cariani PA (2004) Human frequency-following response: representation of pitch contours in Chinese tones. Hearing Research 189:1-12.

Krishnan A, Xu Y, Gandour J, & Cariani P (2005) Encoding of pitch in the human brainstem is sensitive to language experience. Cognitive Brain Research 25(1):161-168.

Krishnan A, Gandour JT, Bidelman GM, Swaminathan J (2009) Experience dependent neural representation of dynamic pitch in the brainstem. Neuroreport 20(4):408.

Kunze T, Hunold A, Haueisen J, Jirsa V, Spiegler A (2016) Transcranial direct current stimulation changes resting state functional connectivity: a large-scale brain network modeling study. NeuroImage 140:174-187.

Lehmann A., Schönwiesner M (2014) Selective attention modulates human auditory brainstem responses: relative contributions of frequency and spatial cues. PloS One 9(1). e85442.

Luke R, De Vos A, Wouters J (2017) Source analysis of auditory steady-state responses in acoustic and electric hearing. NeuroImage 147:568-576.

Mai G, Tuomainen J, Howell P (2018) Relationship between speech-evoked neural responses and perception of speech in noise in older adults. The Journal of the Acoustical Society of America 143(3):1333-1345.

Mai G, Schoof T, Howell P (2019) Modulation of phase-locked neural responses to speech during different arousal states is age-dependent. NeuroImage 189:734-744.

Mathys C, Loui P, Zheng X, Schlaug G (2010) Non-invasive brain stimulation applied to Heschl's gyrus modulates pitch discrimination. Frontiers in Psychology 1:193.

Matsushita R, Andoh J, Zatorre RJ (2015) Polarity-specific transcranial direct current stimulation disrupts auditory pitch learning. Frontiers in Neuroscience 9:174.

Musacchia G, Sams M, Skoe E, Kraus N (2007) Musicians have enhanced subcortical auditory and audiovisual processing of speech and music. Proceedings of the National Academy of Sciences 104(40):15894-15898.

Nitsche M, Paulus W (2001) Sustained excitability elevations induced by transcranial DC motor cortex stimulation in humans. Neurology 57(10):1899-1901.

Oldfield RC (1971) The assessment and analysis of handedness: the Edinburgh inventory. Neuropsychologia 9(1):97-113.

Parbery-Clark A, Marmel F, Bair J, Kraus N (2011) What subcortical–cortical relationships tell us about processing speech in noise. European Journal of Neuroscience 33(3):549-557.

Patterson RD, Uppenkamp S, Johnsrude IS, Griffiths TD (2002) The processing of temporal pitch and melody information in auditory cortex. Neuron 36(4):767-776.

Penagos H, Melcher JR, Oxenham AJ (2004) A neural representation of pitch salience in nonprimary human auditory cortex revealed with functional magnetic resonance imaging. Journal of Neuroscience 24(30):6810-6815.

Presacco A, Simon JZ, Anderson S (2016) Evidence of degraded representation of speech in noise, in the aging midbrain and cortex. Journal of Neurophysiology 116(5):2346-2355.

Puschmann S, Uppenkamp S, Kollmeier B, Thiel CM (2010) Dichotic pitch activates pitch processing centre in Heschl's gyrus. NeuroImage 49(2):1641-1649.

Ranieri F, Podda MV, Riccardi E, Frisullo G, Dileone M, Profice P, Pilato F, Di Lazzaro V, Grassi C (2012) Modulation of LTP at rat hippocampal CA3-CA1 synapses by direct current stimulation. Journal of Neurophysiology, 107(7):1868-1880.

Reato D, Rahman A, Bikson M, Parra LC (2010) Low-intensity electrical stimulation affects network dynamics by modulating population rate and spike timing. Journal of Neuroscience 30(45):15067-15079.

Ross B, Picton TW, Pantev C (2002) Temporal integration in the human auditory cortex as represented by the development of the steady-state magnetic field. Hearing Research 165:68-84.

Ross B, Herdman AT, Pantev C (2005) Right hemispheric laterality of human 40 Hz auditory steady-state responses. Cerebral Cortex 15(12):2029-2039.

Russo NM, Skoe E, Trommer B, Nicol T, Zecker S, Bradlow A, Kraus N (2008) Deficient brainstem encoding of pitch in children with autism spectrum disorders. Clinical Neurophysiology 119(8):1720-1731.

Salehinejad M, Kuo M, Nitsche M (2019) The impact of chronotypes and time of the day on tDCS-induced motor cortex plasticity and cortical excitability. Brain Stimulation 12(2):421.

Schochat E, Rocha-Muniz CN, Filippini R (2017) Understanding auditory processing disorder through the FFR. In: The Frequency-Following Response: A Window into Human Communication (Kraus N, Anderson S,, White-Schwoch T, Fay RR, Popper AN, eds), pp225-250. Springer, Cham.

Sehm B, Schäfer A, Kipping J, Margulies D, Conde V, Taubert M, Villringer A, Ragert P (2012) Dynamic modulation of intrinsic functional connectivity by transcranial direct current stimulation. Journal of Neurophysiology 108(12):3253-3263.

Shah B, Nguyen TT, Madhavan S (2013) Polarity independent effects of cerebellar tDCS on short term ankle visuomotor learning. Brain Stimulation 6(6):966-968.

Skoe E, Kraus N (2010) Auditory brainstem response to complex sounds: a tutorial. Ear and Hearing 31(3):302.

Skoe E, Chandrasekaran B, Spitzer ER, Wong PC, Kraus N (2014) Human brainstem plasticity: the interaction of stimulus probability and auditory learning. Neurobiology of Learning and Memory 109:82-93.

Smalt CJ, Krishnan A, Bidelman GM, Ananthakrishnan S, Gandour JT (2012) Distortion products and their influence on representation of pitch-relevant information in the human brainstem for unresolved harmonic complex tones. Hearing Research 292:26-34.

Song JH, Skoe E, Banai K, Kraus N (2011) Perception of speech in noise: neural correlates. Journal of Cognitive Neuroscience 23(9):2268-2279.

Stagg CJ, Best JG, Stephenson MC, O'Shea J, Wylezinska M, Kincses ZT, Morris PG, Matthews PM, Johansen-Berg H (2009) Polarity-sensitive modulation of cortical neurotransmitters by transcranial stimulation. Journal of Neuroscience 29(16):5202-5206.

Strait DL, Kraus N, Skoe E, Ashley R (2009) Musical experience and neural efficiency: effects of training on subcortical processing of vocal expressions of emotion. European Journal of Neuroscience 29:661–668.

Unal G, Bikson M (2018) Transcranial Direct Current Stimulation (tDCS). In: Neuromodulation: Comprehensive Textbook of Principles, Technologies, and Therapies (Krames E, Peckham PH, Rezai AR, eds), pp1589-1610, Academic Press.

Vanvooren S, Hofmann M, Poelmans H, Ghesquière P, Wouters J (2015) Theta, beta and gamma rate modulations in the developing auditory system. Hearing Research 327:153-162.

White-Schwoch T, Carr KW, Thompson EC, Anderson S, Nicol T, Bradlow AR, Zecker SG, Kraus N (2015) Auditory processing in noise: A preschool biomarker for literacy. PLoS Biology 13(7):e1002196

Willems RM, Van der Haegen L, Fisher SE, Francks C (2014) On the other hand: including left-handers in cognitive neuroscience and neurogenetics. Nature Reviews Neuroscience 15(3):193-201.

Wong PC, Skoe E, Russo NM, Dees T, Kraus N (2007) Musical experience shapes human brainstem encoding of linguistic pitch patterns. Nature Neuroscience 10(4):420-422.

Zatorre RJ, Belin P (2001) Spectral and temporal processing in human auditory cortex. Cerebral Cortex 11(10):946-953.